

A comparative study of target volumes based on ^{18}F -FDG PET-CT and ten phases of 4DCT for primary thoracic squamous esophageal cancer

Yanluan Guo
Jianbin Li
Peng Zhang
Yingjie Zhang

Department of Radiation Oncology
(Chest Section), Shandong Cancer
Hospital and Institute, Jinan, Shandong
Province, People's Republic of China

Purpose: To investigate the correlations in target volumes based on ^{18}F -FDG PET/CT and four-dimensional CT (4DCT) to detect the feasibility of implementing PET in determining gross target volumes (GTV) for tumor motion for primary thoracic esophageal cancer (EC).

Methods: Thirty-three patients with EC sequentially underwent contrast-enhanced 3DCT, 4DCT, and ^{18}F -FDG PET-CT thoracic simulation. The internal gross target volume (IGTV)₁₀ was obtained by combining the GTV from ten phases of 4DCT. The GTVs based on PET/CT images were defined by setting of different standardized uptake value thresholds and visual contouring. The difference in volume ratio, conformity index (CI), and degree of inclusion (DI) between IGTV₁₀ and GTV_{PET} was compared.

Results: The images from 20 patients were suitable for further analysis. The optimal volume ratio of 0.95 ± 0.32 , 1.06 ± 0.50 , 1.07 ± 0.49 was at standardized uptake value (SUV)_{2.5}, SUV_{20%}, or manual contouring. The mean CIs were from 0.33 to 0.54. The best CIs were at SUV_{2.0} (0.51 ± 0.11), SUV_{2.5} (0.53 ± 0.13), SUV_{20%} (0.53 ± 0.12), and manual contouring (0.54 ± 0.14). The mean DIs of GTV_{PET} in IGTV₁₀ were from 0.60 to 0.90, and the mean DIs of IGTV₁₀ in GTV_{PET} ranged from 0.35 to 0.78. A negative correlation was found between the mean CI and different SUV ($P=0.000$).

Conclusion: None of the PET-based contours had both close spatial and volumetric approximation to the 4DCT IGTV₁₀. Further evaluation and optimization of PET as a tool for target identification are required.

Keywords: esophageal cancer, ^{18}F -FDG PET/CT, four-dimensional computed tomography, contour, tumor motion

Introduction

Currently, radiotherapy is one of the most important treatment modalities for patients with esophageal cancer (EC), but it is associated with poor therapeutic effect. The overall 5-year survival rate for patients treated with conventional doses of radiotherapy alone is below 10%.^{1,2} Local recurrence is one of the main causes of treatment failure. The main reason for local failure after radiotherapy is the inability to precisely define accurate target volumes.

The majority of patients with EC are treated during free respiration. In this state, EC motion can be attributed to respiration, cardiac activity, and peristalsis.³ Therefore, it is necessary to investigate the methods of tumor motion to improve the accuracy of target volume delineation in the image for radiation treatment planning.

Four-dimensional CT (4DCT) has been considered as an effective tool for assessing tumor and organ motion.⁴⁻⁶ One approach to define tumor motion is to contour gross target

Correspondence: Jianbin Li
Department of Radiation Oncology,
Shandong Cancer Hospital and Institute,
440 Jiyuan Road, Jinan 250117,
People's Republic of China
Tel +86 531 6762 6131
Fax +86 531 6762 6130
Email lijianbin@msn.com

volumes (GTVs) on ten phases of 4DCT and obtain internal gross target volume (IGTV) by combining them; theoretically, this would give information about the entire tumor motion.^{7,8}

A free-breathing PET (FB-PET) scan is performed in multiple bed steps for 2–5 minutes; it represents a time-averaged map of the tumor position. The blurred target outline on the FB PET scan could help to define the internal target volume (ITV).⁹ Theoretically, for PET images, the high contrast between tumor and background indicates that even long acquisitions do not result in the tumor being lost in the background. Phantom studies have supported this theory,^{10,11} but there are no clinical data that validate it.

Considering that both FBPET and 4DCT could help to define an ITV, it seems logical to compare PET thresholds to 4DCT to determine an optimal segmentation method. Despite the fact that respiratory 4D PET-CT techniques are highly useful in target volume delineation¹² (accurately representative of organ and lesion motion), the feasibility of implementing it in determining the GTV for EC is still unknown. 3DPET-CT, integrated with 4DCT, might be selected as an alternative. It is necessary to study the relevance between the FB 3DPET-based GTVs and 4DCT-based targets in determining target motion in radiation treatment. Ten delineation methods were used to define the best volume fit between the two different modality-based target volumes for EC.

Materials and methods

Patient selection and characteristics

Patients with pathologically proven EC scheduled to accept radiotherapy were consecutively enrolled. None of them had been treated with radiotherapy or chemotherapy before. Thirty-one patients with EC were selected between November 2012 and November 2014. The patients with maximal standardized uptake value (SUV) on PET of less than 2.0 were excluded. Totally, the data from 20 patients were available for investigation. The patient characteristics are listed in Table 1.

CT acquisition

During the simulation, all patients were fixed in a relatively stable position using a thermoplastic mask and by placing their arms on the side of the body. For each patient, an axial enhanced 3DCT scan of the thoracic region was performed, followed by an enhanced 4DCT scan under uncoached FB conditions on a 16-slice CT scanner (Philips Brilliance Bores CT, Philips, the Netherlands) with the administration of intravenous contrast agents. A total of 100 mL of ioversol was injected intravenously, 2 mL/s for 3DCT, and 1 mL/s for 4DCT. The 3DCT and 4DCT data sets were acquired from the 20 patients on a 16-slice CT scanner (Philips Brilliance Bores CT) during FB. Three laser alignment lines were marked on the patient before CT

Table 1 The characteristics of the patients enrolled in the study

Patients	Sex	Age (years)	Tumor location	SUV _{max}	Pathologic type	TNM stage
1	Female	77	Middle	19.39	Squamous	T2N1Mx
2	Male	69	Distal	9.33	Squamous	T3N2M0
3	Female	57	Middle	9.71	Squamous	T2N1M0
4	Male	74	Middle	12.29	Squamous	T3N1M0
5	Female	66	Distal	11.82	Squamous	T1N1M0
6	Female	74	Middle	10.41	Squamous	T2N1M0
7	Male	53	Upper	17.39	Squamous	T2N0M0
8	Male	71	Distal	30.46	Squamous	T3N2Mx
9	Male	62	Distal	17.2	Squamous	T2N2M0
10	Female	58	Middle	14.55	Squamous	T2N1M0
11	Male	80	Middle	15.98	Squamous	T2N0Mx
12	Male	68	Distal	15.32	Squamous	T3N2M0
13	Male	44	Distal	9.13	Squamous	T3N1M0
14	Male	58	Upper	13.67	Squamous	T2N1M0
15	Male	63	Middle	7.40	Squamous	T3N0M0
16	Female	52	Upper	19.85	Squamous	T4N1M0
17	Male	71	Distal	15.57	Squamous	T2N1Mx
18	Male	57	Middle	11.96	Squamous	T3N2Mx
19	Male	44	Upper	9.36	Squamous	T3N2M0
20	Male	65	Upper	11.87	Squamous	T2N1M0

Note: "x" = distant metastasis unknown.

Abbreviation: SUV, standardized uptake value.

acquisition. The 3DCT scan, in which 12 contiguous slices with a thickness of 3 mm thickness were produced per gantry rotation (1 s) and interval (1.8 s) between rotations, was acquired in sequential mode, and the 4DCT scan was acquired in helical mode with the scanning pitch between 0.09 and 0.15. The respiratory signal was recorded with the Varian real-time position management system (Varian Medical Systems, Palo Alto, CA, USA), by measuring the displacement of the infrared markers placed on the epigastric region of the patient's abdomen. GE Advantage 4D software (GE Healthcare, Waukesha, WI, USA) was used to sort the reconstructed 4DCT images into ten respiratory phases labeled as 0%–90% on the basis of triggered signal. Phase 0% denoted the maximum end inspiration and phase 50% denoted the maximum end expiration. The 4DCT images were reconstructed using a thickness of 3 mm.

PET-CT image acquisition

On the same day as the 4DCT scan, the ^{18}F -FDG-PET/CT scans of the chest were performed with an integrated PET/CT scanner (Philips Gemini TF Big Bore). Using the same immobilization devices, the patient was positioned identical to that for the 4DCT scan. Two radiation therapists were present to ensure the accuracy of the setup, assessed using a laser localizer and skin marks. All patients fasted for at least 6 hours before the PET/CT examination. All patients were injected with 7.4 MBq/kg body weight of ^{18}F -FDG and then rested for approximately 1 hour in a quiet room before imaging. The 16-slice CT component was operated with an X-ray tube voltage peak of 120 kV, 90 mA, a slice thickness of 5 mm, and an interval of 4 mm and was used both for attenuation correction of PET data and for localization of ^{18}F -FDG uptake in PET images. No CT contrast agent was administered. PET scanning was performed covering the same axial range for 2 minutes per bed position (total of 3–5 bed positions). Both PET and CT acquisition was performed during FB. Data were reconstructed using an ordered subset expectation maximization algorithm and attenuation correction derived from CT data. Then, the PET/CT images were transferred to MIM software (Cleveland, OH, USA).

Image registration

All the image data were transferred into MIM. An initial automatic rigid registration was performed. Because the 3DCT and 4DCT images for the same person were produced during the same imaging session, MIM would consider the

images as being registered with each other. After the image data sets were coregistered with the help of the transmission CT from PET/CT, the 4DCT images will be autoregistered with the CT component of PET/CT.

PET-CT and CT target volume delineation and data acquisition

The targets in our study were contoured by the same senior radiotherapist; the radiotherapist underwent a strict training and contoured the targets following the same standard: The GTVs of different phases were delineated using the same window width and window level following the standards of an esophageal wall thickness >5 mm or an esophageal wall diameter (without gas) >10 mm. We could not ignore the error in the intraobserver by manual contouring. Before the formal contouring, we did a test: The radiotherapist contoured the targets two times in 6 patients (2 in the upper, 2 in the middle, and 2 in the distal, randomly) 2 weeks apart; the results are listed in Table 2. No significant differences were observed between the two times.

Therefore, our results would be less affected by the manual contouring intraobserver errors.

GTVs were manually contoured on the ten phases of the 4DCT images using mediastinal window setting (window width =400 HU, window level =40 HU). IGTV_{10} were obtained by combining GTVs contoured on ten phases of 4DCT. PET/CT-based GTVs of the primary tumor were automatically contoured by using nine different methods: $\text{SUV} \geq 2.0$, ≥ 2.5 , ≥ 3.0 , ≥ 3.5 ; $\geq 20\%$, $\geq 25\%$, $\geq 30\%$, $\geq 35\%$, $\geq 40\%$ of the maximum SUV_{max} , and visual contouring. The methods were determined by the results of other references.^{10,13–16} All the noncancerous regions within the GTV_{PET} , including the areas overlaid by the heart, bone, and great vessels, were corrected to exclude manually with the help of the CT component of PET/CT. The target volumetric size, the centroid coordinates for PET contours, and IGTV_{10} can be determined by MIM. Figure 1 shows an example of the GTV delineated in the text.

Table 2 The variation of intraobserver for the comparison of the GTV volume between different times (cm^3)

Time	Upper	Middle	Lower	Overall			
First	19.22	12.32	20.28	69.44	38.07	24.11	30.57±8.52
Second	23.51	9.93	24.35	71.07	39.77	28.33	32.83±8.59
P-value	–	–	–	–	–	–	P=0.086

Abbreviation: GTV, gross target volume.

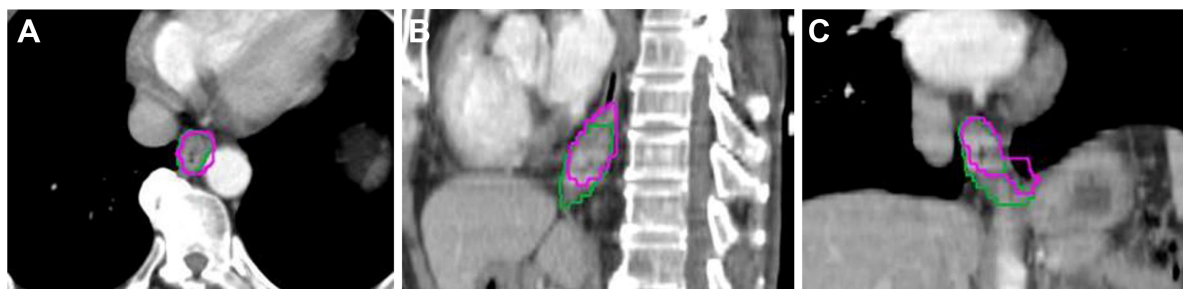


Figure 1 An example of the contours delineated in the image sessions in transversal (A), sagittal (B), and coronal section (C).

Note: The pink contour represents the GTV on $SUV_{20\%}$ and the green one represents $IGTV_{10}$.

Abbreviations: GTV, gross target volume; SUV, standardized uptake value.

Target volume centroid distance

Then target centroid shift in the left–right (LR), anterior–posterior (AP), and cranial–caudal (CC) directions between GTV_{PET} and $IGTV_{10}$ was obtained as Δx , Δy , and Δz , respectively. The centroid distance was calculated as follows:

$$V = (\Delta x^2 + \Delta y^2 + \Delta z^2)^{1/2}$$

Volume ratio, conformity index, and degree of inclusion

To compare GTV_{PET} based on PET-CT and $IGTV_{10}$ based on 4DCT, three measures were used: volume ratio (VR), conformity index (CI), and degree of inclusion (DI). The VR is the ratio of two volumes. The conformity index of volume A and B [CI (A, B)] was defined as the ratio of the intersection of A with B to the union of A and B.¹³ The maximum value of CI is 1 if the two volumes are identical, and the minimum value is 0 if the volumes are completely nonoverlapping. That is,

$$CI = A \cap B / A \cup B$$

The definition of DI of volume A included in volume B, [DI (A in B)], is the intersection between volume A and volume B divided by volume A. The formula is as follows:⁷

$$DI (A \text{ in } B) = A \cap B / A$$

Statistical analysis

The SPSS software package (SPSS 17.0, Chicago, IL, USA) was performed for statistical analysis. Descriptive statistics were used as appropriate. The paired sample Student's *t*-test and Wilcoxon test was used for comparison of tumor position, volumetric size, CI, and DI. Values of $P < 0.05$ were regarded as significant.

Results

The variations of target centroid shift between $IGTV_{10}$ and GTV_{PET}

Table 3 lists the target centroid shift in LR, AP, CC, and 3D directions. In CC direction, the centroid coordinates of all GTV_{PET} showed statistical significance to that of $IGTV_{10}$ ($P > 0.05$), while the GTV_{PET} in other directions differed no significantly to that of $IGTV_{10}$ ($P < 0.05$).

Table 3 The target centroid shift between GTV_{PET} and $IGTV_{10}$ in LR, AP, and CC directions, and 3D represents the centroid distance between GTV_{PET} and $IGTV_{10}$ (mean \pm SD, and median, mm)

Target terms	LR	AP	CC	Centroid distance
$SUV_{2.0}$	-0.39 ± 1.99 (–0.15)	0.37 ± 1.70 (0.45)	3.33 ± 6.26 (1.45)	5.73 ± 4.83 (4.06)
$SUV_{2.5}$	-0.65 ± 1.99 (–0.53)	0.73 ± 1.86 (0.50)	3.24 ± 6.71 (2.15)	6.55 ± 4.40 (5.63)
$SUV_{3.0}$	-0.63 ± 2.20 (–0.46)	0.74 ± 1.99 (0.40)	2.48 ± 6.13 (1.95)	5.78 ± 4.32 (4.43)
$SUV_{3.5}$	-0.58 ± 2.26 (–0.66)	0.65 ± 1.99 (0.45)	2.61 ± 6.75 (1.70)	6.00 ± 4.93 (4.10)
$SUV_{20\%}$	-0.28 ± 2.02 (0.05)	0.45 ± 1.50 (0.50)	2.63 ± 6.69 (1.70)	5.87 ± 4.73 (4.02)
$SUV_{25\%}$	-0.59 ± 2.25 (–0.45)	0.69 ± 1.90 (0.45)	3.44 ± 6.84 (2.25)	6.54 ± 7.74 (2.50)
$SUV_{30\%}$	-0.81 ± 2.36 (–1.23)	0.64 ± 1.95 (0.35)	2.75 ± 6.53 (2.35)	6.22 ± 4.53 (5.10)
$SUV_{35\%}$	-0.78 ± 2.31 (–1.30)	0.58 ± 2.08 (0.40)	2.41 ± 6.53 (1.95)	6.07 ± 4.53 (4.85)
$SUV_{40\%}$	-0.88 ± 2.37 (1.35)	0.56 ± 2.25 (0.50)	2.12 ± 6.20 (1.75)	5.91 ± 4.26 (4.92)
Manual contouring	-0.77 ± 1.85 (–0.70)	0.70 ± 2.38 (0.62)	2.66 ± 5.60 (1.83)	5.21 ± 4.57 (4.53)

Abbreviations: GTV, gross target volume; LR, left–right; AP, anterior–posterior; CC, cranial–caudal; SUV, standardized uptake value.

Table 4 The VR, DI, and CI of GTV_{PET} and IGTV₁₀ (mean ± SD and median)

Parameters	VR	DIs of GTV _{PET} and IGTV ₁₀		CI
		IGTV ₁₀ in GTV _{PET}	GTV _{PET} in IGTV ₁₀	
SUV _{2.0}	1.35±0.42 (1.30)	0.78±0.14 (0.83)	0.60±0.13 (0.16)	0.51±0.11 (0.50)
SUV _{2.5}	0.95±0.32 (0.93)	0.67±0.17 (0.72)	0.73±0.11 (0.74)	0.53±0.13 (0.54)
SUV _{3.0}	0.74±0.29 (0.74)	0.58±0.20 (0.65)	0.81±0.10 (0.84)	0.50±0.15 (0.53)
SUV _{3.5}	0.62±0.28 (0.65)	0.52±0.21 (0.59)	0.86±0.09 (0.88)	0.46±0.17 (0.51)
SUV _{20%}	1.06±0.50 (0.86)	0.69±0.12 (0.68)	0.72±0.18 (0.77)	0.53±0.12 (0.55)
SUV _{25%}	0.74±0.26 (0.68)	0.58±0.13 (0.61)	0.81±0.13 (0.85)	0.51±0.12 (0.51)
SUV _{30%}	0.56±0.17 (0.57)	0.49±0.12 (0.50)	0.87±0.10 (0.90)	0.45±0.11 (0.46)
SUV _{35%}	0.45±0.13 (0.46)	0.41±0.12 (0.42)	0.90±0.08 (0.92)	0.39±0.11 (0.40)
SUV _{40%}	0.37±0.13 (0.37)	0.35±0.12 (0.34)	0.79±0.26 (0.93)	0.33±0.11 (0.33)
Manual contouring	1.07±0.49 (1.13)	0.74±0.20 (0.82)	0.75±0.26 (0.74)	0.54±0.14 (0.58)

Abbreviations: GTV, gross target volume; SUV, standardized uptake value; VR, volume ratio; CI, conformity index; DI, degree of inclusion; SD, standard deviation.

Variations in VR, CI, and DI

The VR, CI, and DI of GTV_{PET} to IGTV₁₀ are listed in Table 4. The best volume match for VR was observed at SUV_{2.5}, SUV_{20%}, or manual contouring, which achieved the optimal VR values of (0.95±0.32), (1.06±0.50), and (1.07±0.49), respectively. The best fit for CI was at (0.51±0.11), SUV_{2.5} (0.53±0.13), SUV_{20%} (0.53±0.12), and manual contouring (0.54±0.14). The mean DIs of GTV_{PET} in IGTV₁₀ were from 0.60 to 0.90, and the mean DI of IGTV₁₀ in GTV_{PET} ranged from 0.35 to 0.78. A negative correlation was observed between nine different mean SUV_{max} (2.0, 2.5, 20% mean SUV_{max}=2.83, 3.0, 3.5, 25% mean SUV_{max}=3.53, 30% mean SUV_{max}=4.24, 35% mean SUV_{max}=4.95, 40% mean SUV_{max}=5.65) and the mean CI (0.51, 0.53, 0.53, 0.50, 0.46, 0.51, 0.45, 0.39, 0.33) ($t=-0.931$, $P=0.000$).

The best VR and CI of the groups of low SUV_{max}, median SUV_{max}, and high SUV_{max}

The threshold may be different between low SUV_{max}, median SUV_{max}, and high SUV_{max}. Therefore, the 20 cases on average were divided into three groups: low SUV_{max} with the six lowest SUV_{max} (7.40, 9.13, 9.33, 9.36, 9.71, 10.41) among the cases, median SUV_{max} (11.82, 11.87, 11.96, 12.29, 13.67, 14.55, 15.32) with the seven median SUV_{max}, and high SUV_{max} with the seven highest SUV_{max} (15.57, 15.98, 17.20, 17.39, 19.39, 19.85, 30.40). Finally, the best VR and CI were recalculated, and these are listed in Table 5.

Table 5 The best VR and CI for low SUV_{max}, median SUV_{max}, and high SUV_{max} groups

Parameters	Low SUV _{max}	Median SUV _{max}	High SUV _{max}
The best SUV value for VR and CI	2, 25% SUV _{max} , manual contouring	2.5, 20% SUV _{max} , manual contouring	3.0, 3.5, manual contouring

Abbreviation: SUV, standardized uptake value.

The best VR and CI of the groups of different locations

The threshold may also be different between different locations. Therefore, the 20 cases on average were divided into three groups: the upper segment group (five cases), the middle segment group (eight cases), and the distal (seven cases). And the best VR and CI were recalculated, in which are listed in Table 6.

Discussion

Chang et al¹⁷ proved that a single static PET/CT scan had the potential to replace a 4DCT to determine the tumor ITV based on an experiment of phantom or peripheral non-small-cell lung cancer patients. In a phantom study, Okubo et al¹⁰ showed that the PET-based ITV approximated to but did not accurately reproduce the maximum intensity projection (MIP) ITV derived from 4DCT. These previous documents focused on the comparison of the ITV based on 4DCT and PET session images by experiments of phantom and peripheral non-small-cell lung cancer patient.^{10,17,18} This research mainly concentrated on the comparison of target volumes for primary EC delineated on PET-CT and ten phases of 4DCT.

In this study, our results suggested that the target volumes contoured at SUV_{2.5}, SUV_{20%}, or visual interpretation matched better with the IGTV that was combined from GTVs contoured on ten phases of 4DCT in VR, CI than other SUV threshold setting methods for all patients. A negative correlation was

Table 6 The best VR and CI for upper, middle, and distal segment groups

Parameters	Upper	Middle	Distal
The best SUV value for VR and CI	2.5, 20% SUV _{max} ^a manual contours	2.5, 20% SUV _{max} ^a manual contours	2.0, 20% SUV _{max} ^a manual contours

Abbreviations: SUV, standardized uptake value; VR, volume ratio; CI, conformity index.

observed between different mean SUV_{max} and the mean CI ($P=0.000$). However, the poor CIs (0.55, 0.56, 0.57) and DIs (range: 0.65–0.77) suggested that great nonconformity between IGTV₁₀ and GTV_{PET}. One of the reasons is that shape and/or positional alterations between IGTV₁₀ and GTV_{PET} had occurred. In CC direction, the centroid coordinates of all GTV_{PET} showed statistical significance to that of IGTV₁₀ (P), while the GTV_{PET} in other directions differed no significantly to that of IGTV₁₀. Thus, these results indicated that geographic miss would come into being and that a large part of normal tissues would be irradiated whether GTV_{PET} or IGTV₁₀ was used as the treatment target volume.

Our results were consistent with some previous documents. Wang et al¹⁶ compared GTV determined from average 4DPET and average 4DCT, and proved that GTV_{PET} at SUV_{2.5}, SUV_{20%} correlated well with GTV_{CT} in tumor length, VR, and CI, but the CIs (0.58, 0.57) were also not ideal. Callahan et al¹⁹ used 4DPET to create “PET-MIP” image sets and segmented PET ITVs at thresholds ranging from 20% to 40% of maximum SUV. The investigators compared these volumes to ITVs drawn by radiation oncologists on the 4DCTMIP and found good overlap between PET-MIP volumes and CT-MIP volumes, but poor overlap between FBPET volumes and CT-MIP volumes.¹⁹ Hanna et al’s¹⁸ work compared ITV determined from FB-PET/CT with modified 4DCT-MIP for 16 patients with NSCLC receiving SABRT using the concordance index (equivalent to CI in our study). The mean concordance index of their study was 0.64 and 0.57 in GTV_{PET-CT} and GTV_{CT}. This indicated that the target volumes derived from FB-PET did not correspond well to those derived from 4DCT-MIP.

Limitations

It should be noted that, in our research, the two limitations that existed in the research by Hanna et al could be avoided. First, considering that the change of tumor geometry or size and a potential increase in the likelihood of a mismatch between IGTV₁₀ and GTV_{PET} because of the treatment or long time interval during PET-CT and 4DCT, all the patients enrolled in this study performed PET-CT and 4DCT simulation scans on the same day without any treatment. Furthermore, keeping the same body position during

the two simulation in our research may reduce more setup errors and the incidence of misregistration between the two simulation scans than the study by Hanna et al¹⁸ in which the PET simulation was performed on a curved table top while the 4DCT simulation on a flat table top. Different from this study, in our previous study, we compared the geometrical differences among planning target volumes (PTV) defined by PET combined with 4DCT, to 3DCT, and 4DCT, respectively, and discovered that PET combined with 4DCT could affect not only the volume of the PTV but also its shape.²⁰ As the esophagus does not strictly run straightly up and down, and the CTV should be constructed by GTV added additional margin of 30 mm in cranial–caudal direction and 5 mm in transversal direction, therefore, the additional margin in the cranial–caudal direction should be contoured along the wall of the esophagus. So the PTV that is formed by CTV is different from the GTV.

As we all know, it is the ratio or gradient between the background ¹⁸F-FDG uptake and tumor uptake that makes any method of PET-based contouring possible.²¹ The size of PET delineation changes significantly depending on its threshold value. To encompass the whole tumor motion shape, the image threshold must be decreased. As mentioned earlier, it indicated that selection of an image threshold that is too low would overestimate the true volume, leading to a risk of increased normal tissue toxicity. Moreover, the method of contouring margins around the target lesion cannot be uniform, which could be verified from different results of the best VR and CI for the groups of low SUV_{max}, median SUV_{max}, and high SUV_{max}.

In another term, esophageal motion due to respiration is important especially for lower tumors. It would be important to note the difference in GTV on phase and the IGTV₁₀ in the patients in relation to location. In this paper, the best threshold between different locations for EC tells us that the SUV might be affected significantly by tumor motion (Table 5). Thus, although a standardized method for optimal PET delineation for RTP has not yet been established, several investigators have reported that the use of single-threshold model for delineating the GTV with PET/CT is not sufficient because of the effects of the target size, motion, and image reconstruction parameters.²²

Other possible explanations for the geometrical mismatch between GTV_{PET} and $IGTV_{10}$ are as follows: 1) Despite the scans being done sequentially, with the patient in the same position throughout, the patient could have moved slightly between scans. A rigid registration might not be sufficient for lung tumors. Hence, registration error may inevitably affect the spatial position between GTV_{PET} and $IGTV_{10}$. 2) Some of this difference may be related to differences in the patient's breathing pattern between acquiring the PET/CT and 4DCT. 3) The false-positive. Thus, at the present time, it is perhaps most appropriate to consider PET as one component of a multimodality approach to target delineation, and we agree with the previous studies that suggested that PET may help to define the presence of tumor for target volume definition purposes, but the edge of the PTV should be defined from 4DCT or conventional CT.²³ 4) The different slice thickness for the 3D and 4D CTs (3 mm) and that of the PET-CT (5 mm) may be responsible for some of the geometrical mismatch. Further evaluation and optimization of PET as a tool for target identification are required.

Conclusion

Using the methods described, ¹⁸F-FDG PET-CT-based target volumes did not correspond well with 4DCT-based target volumes. None of the PET-based contours had both close spatial and volumetric approximation to the 4DCT $IGTV_{10}$ for EC.

Acknowledgment

The authors acknowledge Dr Jinming Yu (Shandong Cancer Hospital and Institute).

Ethical approval

All patients provided signed informed consent to participate in the study and before undergoing further imaging during radiotherapy. The study design was approved by the ethics committee of Shandong Cancer Hospital and Institute.

The ethics committee of Shandong Cancer Hospital and Institute conformed to the code of Ethics of the World Medical Association.

Disclosure

The authors report no conflicts of interest in this work.

References

1. Sun DR. Ten year follow-up of esophageal cancer treated by radical radiation therapy: analysis of 869 patients. *Int J Radiat Oncol Biol Phys.* 1989;16(2):329–334.
2. Okawa T, Kita M, Tanaka M, Ikeda M. Results of radiotherapy for inoperable locally advanced esophageal cancer. *Int J Radiat Oncol Biol Phys.* 1989;17(1):49–54.

3. Hashimoto T, Shirato H, Kato M, et al. Real-time monitoring of a digestive tract marker to reduce adverse effects of moving organs at risk (OAR) in radiotherapy for thoracic and abdominal tumors. *Int J Radiat Oncol Biol Phys.* 2005;61(5):1559–1564.
4. Keall PJ, Starkschall G, Shukla H, et al. Acquiring 4D thoracic CT scans using a multislice helical method. *Phys Med Biol.* 2004;49(10):2053–2067.
5. Dinkel J, Welzel T, Bolte H, et al. Four-dimensional multislice helical CT of the lung: qualitative comparison of retrospectively gated and static images in an ex-vivo system. *Radiother Oncol.* 2007;85(2):215–222.
6. Patel AA, Wolfgang JA, Niemierko A, Hong TS, Yock T, Choi NC. Implications of respiratory motion as measured by four-dimensional computed tomography for radiation treatment planning of esophageal cancer. *Int J Radiat Oncol Biol Phys.* 2009;74(1):290–296.
7. Li F, Li J, Zhang Y, et al. Geometrical differences in gross target volumes between 3DCT and 4DCT imaging in radiotherapy for non-small-cell lung cancer. *J Radiat Res.* 2013;54(5):950–956.
8. Wang W, Li JB, Zhang YJ, et al. Comparison of patient-specific internal gross tumor volume for radiation treatment of primary esophageal cancer based separately on three-dimensional and four-dimensional computed tomography images. *Dis Esophagus.* 2014;27:348–354.
9. MacManus M, Nestle U, Rosenzweig KE, et al. Use of PET and PET/CT for radiation therapy planning: IAEA expert report 2006–2007. *Radiother Oncol.* 2009;91(1):85–94.
10. Okubo M, Nishimura Y, Nakamatsu K, et al. Static and moving phantom studies for radiation treatment planning in a positron emission tomography and computed tomography (PET/CT) system. *Ann Nucl Med.* 2008;22(7):579–586.
11. Riegel AC, Bucci MK, Mawlawi OR, Johnson V, Ahmad M, Sun X. Target definition of moving lung tumors in positron emission tomography: correlation of optimal activity concentration thresholds with object size, motion extent, and source-to-background ratio. *Med Phys.* 2010;37:1742–1752.
12. Bettinardi V, Picchio M, Di Muzio N, et al. Detection and compensation of organ/lesion motion using 4D-PET/CT respiratory gated acquisition techniques. *Radiother Oncol.* 2010;96(3):311–316.
13. Vali FS, Nagda S, Hall W, et al. Comparison of standardized uptake value-based positron emission tomography and computed tomography target volumes in esophageal cancer patients undergoing radiotherapy. *Int J Radiat Oncol Biol Phys.* 2010;78(4):1057–1063.
14. Zhong X, Yu J, Zhang B, et al. Using 18F-fluorodeoxyglucose positron emission tomography to estimate the length of gross tumor in patients with squamous cell carcinoma of the esophagus. *Int J Radiat Oncol Biol Phys.* 2009;73(1):136–141.
15. Han D, Yu J, Yu Y, et al. Comparison of (18) F-fluorothymidine and (18) F-fluorodeoxyglucose PET/CT in delineating gross tumor volume by optimal threshold in patients with squamous cell carcinoma of thoracic esophagus. *Int J Radiat Oncol Biol Phys.* 2010;76(4):1235–1241.
16. Wang YC, Hsieh TC, Yu CY, et al. The clinical application of 4D 18F-FDG PET/CT on gross tumor volume delineation for radiotherapy planning in esophageal squamous cell cancer. *J Radiat Res.* 2012;53(4):594–600.
17. Chang G, Chang T, Pan T, Clark JW, Mawlawi OR. Determination of internal target volume from a single positron emission tomography/computed tomography scan in lung cancer. *Int J Radiat Oncol Biol Phys.* 2012;83(1):459–466.
18. Hanna GG, van Sörnsen de Koste JR, Dachele MR, et al. Defining target volumes for stereotactic ablative radiotherapy of early-stage lung tumours: a comparison of three-dimensional 18F-fluorodeoxyglucose positron emission tomography and four-dimensional computed tomography. *Clin Oncol.* 2012;24:e71–e80.
19. Callahan J, Kron T, Schneider-Kolsky M, et al. Validation of a 4D-PET maximum intensity projection for delineation of an internal target volume. *Int J Radiat Oncol Biol Phys.* 2013;86(4):749–754.

20. Guo Y-L, Li J-B, Shao Q, Li Y-K, Zhang P. Comparative evaluation of CT-based and PET/4DCT-based planning target volumes in the radiation of primary esophageal cancer. *Int J Clin Exp Med*. 2015;8(11):21516–21524.
21. Davis JB, Reiner B, Huser M, Burger C, Székely G, Ciernik IF. Assessment of 18F PET signals for automatic target volume definition in radiotherapy treatment planning. *Radiother Oncol*. 2006;80(1):43–50.
22. Biehl KJ, Kong FM, Dehdashti F, et al. 18F-FDG PET definition of gross tumor volume for radiotherapy of non-small cell lung cancer: is a single standardized uptake value threshold approach appropriate? *J Nucl Med*. 2006;47(11):1808–1812.
23. Pan T, Mawlawi O. PET/CT in radiation oncology. *Med Phys*. 2008;35(11):4955–4966.

OncoTargets and Therapy

Publish your work in this journal

OncoTargets and Therapy is an international, peer-reviewed, open access journal focusing on the pathological basis of all cancers, potential targets for therapy and treatment protocols employed to improve the management of cancer patients. The journal also focuses on the impact of management programs and new therapeutic agents and protocols on

Submit your manuscript here: <http://www.dovepress.com/oncotargets-and-therapy-journal>

patient perspectives such as quality of life, adherence and satisfaction. The manuscript management system is completely online and includes a very quick and fair peer-review system, which is all easy to use. Visit <http://www.dovepress.com/testimonials.php> to read real quotes from published authors.

Dovepress